Nanocrystalline MoS_2 through Directional Growth along the (002) Crystal Plane under High Pressure

Wang Shanmin, He Duanwei

(Institute of Atomic and Molecular Physics, Sichuan University, ChengDu 610065)

Abstract: The directional growth experiments of graphite-like structured MoS_2 crystallites have been conducted by utilizing a designed sample cell assembly under high pressure (2.0 and 5.0 GPa) and high temperature (700 ºC). X-ray diffraction (XRD) and scanning electron microscope (SEM) are used to characterize the samples. The results show that the prepared nanocrystalline MoS_2 (n-MoS_2) crystals have a hexagonal layered structure. The crystal is uncovered to grow preferentially along the (002) plane, indicating that the low-energy surface is the (002) plane of the crystal. The striking diffuse/broadening nature of Bragg reflection is also analyzed in details, and considered to be associated with the defect structures of the layers stacking and rotational disorder. Measurements of crystallite/grain size are performed by using XRD technique and SEM observation. The measurement results suggest that the traditional peak broadening analysis techniques, including Williamson-Hall formula and Scherrer equation, may not be suitable for the present poorly crystallized n-MoS_2 situation. The results may be conducive to have an insight into the growth mechanism and defects analysis of the layer-structured materials.

Keywords:high pressure; crystal growth; defects; nanostructures

0 Introduction

MoS_2 belongs to the layered transition metal dichalcogenide crystals. The interlayer of the crystal, named ‘sandwich’ structure, consists of one plane of hexagonally packed metal atoms between two planes of chalcogenide atoms. It has attracted interest for applications in catalytic hydrodesulphurization [1-3], solid lubricant [4-5], and intercalation chemistry [6-8]. Although traditional synthesis methods of MoS_2 have been described in the literature [9-12], the growth mechanism of this graphite-like structured crystal remains poorly understood [13]. MoS_2 crystallite possesses a strong bonding within the sandwiches and weak interlayer interactions which originated from loosely bound *Van der Waals* forces. Thus it is theoretically considered that the (002) plane, which parallels the sandwich layer, is the lowest-energy plane. But the experimental evidence for this theoretical supposition has been rarely reported. Interestingly, a poorly crystallized MoS_2 always happens in the traditional synthetic routes [9-12]. This highly disordered crystal is found to have unique properties not present in their corresponding crystalline phases [1-4, 14]. And the defect structures have captured the attention of the scientists and technologists [11, 12, 15-17]. Even though significant knowledge has been gained regarding the defect structure of MoS_2, some aspects still remain puzzling or simply unknown, especially the striking diffuse/broadening nature of the (*h0l*) Bragg reflections.

In this work, poorly crystallized *n*-MoS_2 crystals are prepared through the reaction between sulfur and molybdenum under high pressure. By using a designed high-pressure sample cell, the (002) plane of the crystal shows a favorable crystal plane for MoS_2 growing along it. Based on the previous theoretical investigations [15-17], the defect structures of the prepared MoS_2 are analyzed in details. It is considered that the significantly diffuse/broadening features of Bragg reflections may be attributed to the stacking and rotational disorder of the layers. Accompanied with the disordered structures, micro strain is induced and cannot be ignored in XRD broadening analysis for grain size measurements. Thus the traditional XRD technique based methods do not seem to be

Foundations: Specialized Research Fund for the Doctoral Program of Higher Education(Grant no. 20070610110)
Brief author introduction:王善民，（1980-），男，博士，高压科学与技术
Correspondance author: 贺端威，（1969-），男，教授，高压科学与技术. E-mail: duanweihe@scu.edu.cn

suitable for this poorly crystallized *n*-MoS_2.

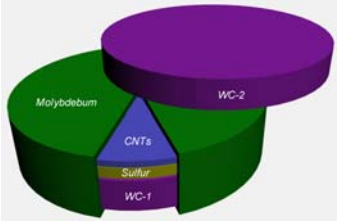

图 1 改进的样品腔体示意图
Fig. 1 Schematic diagram of the designed cell assembly

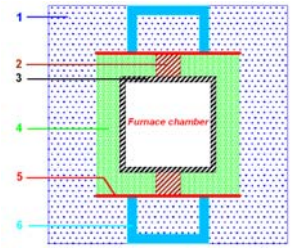

图 2 高压腔体组装: (1)叶腊石,(2)碳柱，(3)石墨加热管，(4)白云石，(5)钼片，(6)钢环
Fig. 2 Schematic diagram of the cell assembly: (1) pyrophyllite, (2) graphite conductor, (3) graphite furnace, (4) dolomite, (5) molybdenum sheet and (6) steel ring

1 Experimental details

1.1 Cell assembly design

High-pressure cell assembly was designed to conduct MoS_2 crystals growth experiments, and details of the cell assembly were described as Fig. 1 shows. Sulfur powder and molybdenum used as the starting materials in the experiments were 99.9% pure. Prior to experiments, sulfur powder was pressed into a disc-shaped pellet, and then encapsulated in a molybdenum container to minimize contamination and sulfur loss during heating process. Apart from as a container, it should be noted that molybdenum also served as a reactant. Carbon nanotubes (*CNTs, >99.5% pure, outer diameter of 8~15 nm and length of ~50 μm*) were selected as a substrate which would not react with sulfur and molybdenum under the present *P-T* conditions. In the experiments, the molten sulfur would infiltrate up through CNTs substrate, and react with molybdenum under high pressure and high temperature (HPHT). The synthesized MoS_2 crystals would directly grow on the surface of CNTs substrate. MoS_2 crystal formation was a sluggish process under the present P-T conditions. Usually, a small amount of molybdenum would be involved in the reaction at the contact surface (see Fig. 1). And the remains still served as a molybdenum container to protect the sample. After taking the remaining molybdenum container off, the as-grown MoS_2 was formed on the CNTs substrate. Two tungsten carbide discs (WC-1 and WC-2) could make the sample have a smooth surface. Thus the synthesized sample would be directly measured by using XRD without other treatments. This could avoid damaging growth information recorded in the sample. The growth information was thus effectively retained and easily revealed by XRD techniques.

1.2 Preparation

The designed assembly illustrated above (see Fig. 1) was encased into a NaCl capsule serving as a pressure-transmitting medium, and then they were put into a sophisticated high-pressure furnace chamber (as Fig. 2 shows) for high-pressure experiments. HPHT experiments were carried out in a DS6×8 MN cubic press [18]. Detailed descriptions of pressure generation and calibration were all reported in our previous literature [19]. The heating and cooling processes were governed

by the power controlling system. And chromel/alumel thermocouple was employed in measurements of temperatures. At a desired pressure (2.0 and 5.0 GPa), temperature was elevated at the desired value (700 ºC) for 15-min heating. Finally, the cell was decompressed slowly to ambient pressure after it was quenched to room temperature.

1.3 Characterization

XRD measurements and SEM observations were used to characterize the as-grown sample. For comparison purposes, the as-grown sample was peeled from the CNTs substrate and then ground into powder shape also for XRD measurements.

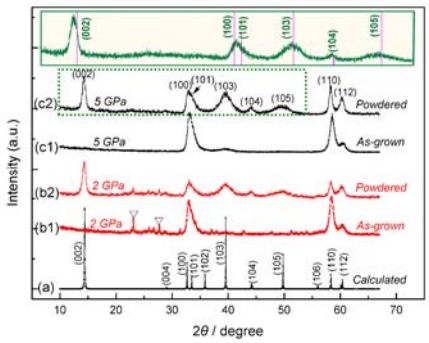

图 3　在 700ºC, 2.0 和 5.0 GPa 下，保温 15min 合成的样品的 XRD 图谱. (a)根据 PDF 卡片(#65-0160)计算的 2*H*-MoS_2 的理论谱. (b1)2.0 GPa 下生长的块体样品，(倒三角代表杂质 S)；(b2）块体样品碾碎后的粉末样品；(c1)，和(c2)分别对应 5.0 GPa 下生长的块体样品和碾碎的粉末样品. 插图为 XRD 谱(c2)的放大部分

Fig. 3 XRD of the samples synthesized at different pressures and temperature of 700 ºC for 15-min heating, (a) The XRD pattern calculated based on PDF data (#65-0160) of 2*H*-MoS_2; (b1) the as-grown crystals synthesized at 2.0 GPa, the inverted triangle represents the sulfur impurity; (b2) powder shaped sample is prepared from the as-grown crystals; and (c1), (c2) correspond to the as-grown and powdered samples, synthesized at 5.0 GPa. The insert box is the enlargement of the selected region in pattern (c2)

2 Results and discussion

Fig. 3 shows XRD measurements of the samples prepared under different pressures of 2.0 and 5.0 GPa. As shown in Fig. 3(b2) and (c2), XRD results of the powdered sample show that the (*h0l*) peaks' broadening is quite different from the others. This implies that the synthesized crystals are characterized as the poorly crystalline disulfides. Similarly, it usually occurs in the traditional synthetic routes [9-12], and the poorly crystallized MoS_2 are mostly considered to be a hexagonal structure (2*H*-MoS_2) [8, 9]. Likewise, what we synthesized in our experiments is also identified as the phase of 2*H*-MoS_2. In fact, molybdenite is known to occur in one of the three structures, including 1*T*- and 3*R*-MoS_2 molytypes [20, 21] other than 2*H* molytype. And phase transitions among these molytypes depending on *P*-*T* conditions are documented in our other paper [22]. Therefore, in this article we will refer to this phase only as 2*H*-MoS_2 or simply MoS_2. Additionally, the calculated XRD pattern of 2*H*-MoS_2 was used as a helpful reference [see Fig. 3(a)].

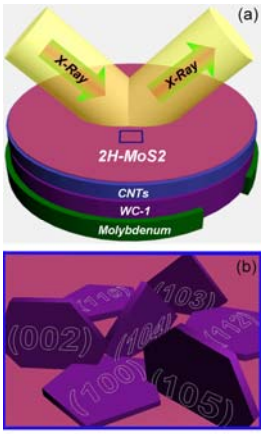

图 4　生长在碳纳米管上面的块体样品的 Bragg 晶面示意图. (a)生长样品的 XRD 测试示意图, (b)对应(a)中选区的放大部分

Fig. 4 Schematic diagram of Bragg planes of the as-grown crystals grown on CNTs substrate. (a) XRD measurements of the synthesized sample without damaging the initial appearance after removing the remaining molybdenum container; (b) the enlargement of a selected region of the as-grown crystals

2.1 Directional growth

Compared with diffraction patterns of the as-grown crystals, the powdered samples exhibit that Bragg reflection of the (002), (103), (104), and (105) planes emerge abruptly (see Fig. 3). An indication that the (110), (100) and (112) planes are lying, while the planes of (002), (103), (104), and (105) are nearly standing vertically on the surface of the CNTs substrate, as Fig. 4 illustrates. It is noted that method of XRD data collection is shown in Fig. 4(a). As described above, the as-grown crystals have been grown on the CNTs substrate without damaging their initial appearances. To better understand our results, a selected region is enlarged as Fig. 4(b) shows. It vividly illustrates the (*hkl*) planes are lying or standing. Obviously, the lying planes can only be captured by XRD tests, while the other cases will be beyond the scopes of the instrument.

The well-defined maxima appearing for the (100), (110), and (112) reflections of the as-grown crystals may contain the growing information of MoS_2 under *P-T* conditions. Fig. 5(a) illustrates crystallographic orientations of the (100), (110), and (112) planes of 2*H*-MoS_2 crystal. These planes are depicted separately for a clear understanding, shown in Fig. 5(b), (c) and (c). It impressed us that the sandwiched interlayers of 2*H*-MoS_2 crystal nearly stand vertically on the CNTs substrate. Thus we consider that 2*H*-MoS_2 crystal has a preferential growth direction along the (002) plane, when sulfur melts and infiltrates up through the substrate to react with molybdenum in the contact region. As we know, crystal growth always happens along the lowest-energy surface of a crystal [23, 24]. Accordingly, the (002) plane possesses the lowest energy in 2*H*-MoS_2 crystal. In fact, the sandwiched interlayers weakly bonded by the *Van der Waals* forces should correspond to a low-energy plane, which is directly observed in our experiments.

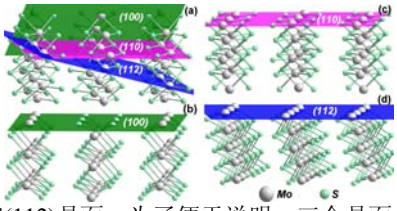

图 5　(100), (110),和(112)晶面，为了便于说明，三个晶面分别对应(a), (b)和(c)

Fig, 5 Crystallographic orientations of the (100), (110), and (112) planes. For better understanding, these planes are depicted in (b), (c) and (d) respectively

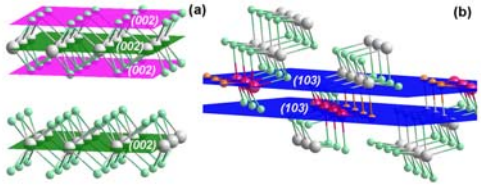

图 6 典型的 (002)和(103) Bragg 平面
Fig. 6 Typical Bragg planes of (002) and (103)

2.2 Peaks broadening/diffuse and shift

As shown in Fig. 3(b2) and (c2), the (103), (104), and (105) peaks look so symmetric diffuse, compared with the (002), (110), and (112) peaks. Bragg scattering from the layer-disordered crystallites has been investigated theoretically [15-17]. And the diffuse natures of the (*h0l*) peaks are mainly considered to be related to the stacking and rotational disorder of the sandwiched layers in MoS_2 crystal [15]. Comparatively, the (002), (100), (110), and (112) peaks are little affected and characterized as a 'normal' broadening caused by crystallite size and instrumental resolution, except that the (100) peak contains the diffused (101) reflection and has an asymmetric shape. Two significantly different XRD diffuse features of the poorly crystallized MoS_2 remain to be explained.

Fig. 6 shows the typical Bragg planes of (002) and (103) for a perfect crystallite. The most striking feature of the (002) reflection is that Bragg scattering arises not only from the inner atoms (including S and Mo) of one sandwich, but also from that of other sandwiches, as shown in Fig. 6(a). However the (103) reflection only originates from fewer atoms coming from different sandwiches. For a crystallite of the poorly crystallized 2*H*-MoS_2, defects such as stacking or rotational disorder of the layers will weaken the diffractions originated from the outer/different sandwiches. The reflections of (h0l) planes thus become so diffuse that it looks like materials with an amorphous structure. Comparatively, the (002), (100), (110), and (112) peaks remain a 'sharper' shape depending on Bragg scattering aroused primarily by atoms of a single sandwich (see Fig. 5 and Fig. 6).

The insert box of Fig. 3 shows that (002) peak is displaced slightly to bigger *d*-values (or smaller 2θ), while other peaks emerge at the proper Bragg positions. This displacement reflects that much macrostrain may be induced in the [002] direction due to the stacking and rotational disorder of the layers.

2.3 Crystallite/grain size

Some well-known standard manners of Bragg pattern broadening analyses are effectively carried out to determine grain size or/and microstrain of a nanosized crystals [25-28]. As shown in Fig. 7, classic Williamson-Hall method is used to calculate crystallite/grain size and microstrain of the prepared *n*-MoS_2. The calculation details see Refs. [26] and [29]. However the data points of the selected (*hkl*) planes look too scattered to conduct linear fitting. Williamson-Hall formula is not suitable for this MoS_2 situation.

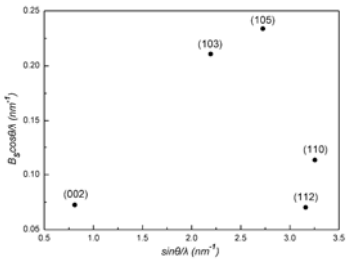

图 7　经典的 Willamos-Hall 方法计算晶粒大小和残余微观应力，粉末样品的制备条件为 2.0 GPa 和 700 ºC
Fig. 7 Classic Williamson-Hall method for grain size and microstrain calculation, the powdered MoS_2 sample was prepared at 2.0 GPa and 700 ºC

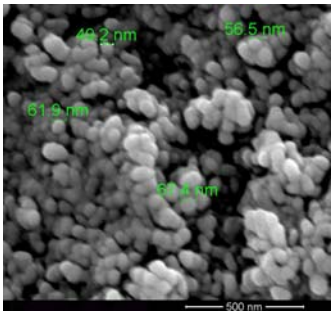

图 8　在 5 GPa、700 ºC 下生长样品的 SEM 图像
Fig. 8 SEM photograph of the as-grown sample prepared under 5.0 GPa and 700 ºC

As discussed above, line broadening arises from a combination factors including the stacking and rotational disorder of the layers, other than the size and strains effects for the current case. Therefore, only Scherrer equation [27, 28] may be suitable for crystallite size measurements from the broadening analysis of a single peak such as the (002), (100), (110), or (112) [see Fig. 3(b2) and (c2)]. And this method has been reported to estimate crystallite size of the similar case of MoS_2 [11, 15]. Table 1 shows that our results of crystallite sizes are estimated from (002) and (110) peaks by using Scherrer equation written as

$$D_{hkl} = \frac{K_{hkl}\lambda}{B_{hkl}\cos\theta}$$

And D_{hkl}, λ, θ, and B_{hkl} are described elsewhere [25, 27]. The constant Khkl depends on the shape of the crystallite. K_{002} and K_{110} are of 0.76 used to estimate D_{002} and D_{110} [15]. Grain size is about 10.0 nm shown in Table 1. But there exists a significant discrepancy compared with the SEM measurements of ~60.0 nm shown in Fig. 8. Undoubtedly, the XRD based results are underrated greatly. The discrepancy is probably attributed to microstrain induced by the defects of layer disorder. And the broadening arises from the defect-induced microstrain without being considered during our measurements. Although the (002) and (110) peaks have a weaker diffuse feature than (h0l) peaks, the defect-induced microstain in the (002) and (110) planes should not be ignored.

表 1　分别从(002)和(110)衍射峰的宽化估算的样品的晶粒大小，样品生长于 2.0 和 5.0 GPa, 为了比较，粉末样品的(110)也用于晶粒的计算
Tab. 1 Crystallite size was estimated by diffraction broadening analysis of the (002) and (110) peaks, respectively, for the crystals grown under different pressures. And the (110) plane of the as-grown crystals were also conducted

	D_{002}	D_{110}	
Pressure	*Powdered*	*Powdered*	*As-grown*
2.0 GPa	10.0 nm	11.9 nm	10.1 nm
5.0 GPa	10.5 nm	12.2 nm	11.0 nm

3 Conclusion

In this paper, 2*H*-MoS_2 crystals are synthesized from the reaction between sulfur and molybdenum under high pressure, by using a designed cell assembly. The XRD measurements show that the crystal prefers to grow along the (002) plane. It implies that the (002) plane has the lowest energy of MoS_2 crystal. Bragg scattering of the (*h0l*) planes are mainly aroused by atoms come from the different sandwiches. Therefore, the interlayer stacking or rotational disorder will weaken the scattering greatly from these atoms of the different layers. While the (002), (100), (110) and (112) planes scatterings primarily originate from atoms within a single sandwich, and will be little affected by those defects. Thus the (*h0l*) peaks look more diffuse than the others. Moreover, the traditional XRD technique based grain size measurement may not be suitable for this *n*-MoS_2 situation, owing to that of the layer disorder induced peak broadening may not be ignored simply.

4 Acknowledgements

This work is funded by the National Natural Science Foundation of China (Grant no. 10772126 & 10976018), and Specialized Research Fund for the Doctoral Program of Higher Education (Grant no. 20070610110).

References

[1] M. Daage, R.R. Chianelli, [J]. J. Catal. 1994, 149: 414.
[2] E. J. M. Hensen, J. A. R. van Veen, [J]. Catal. Today. 2003, 86: 87.
[3] J. V. Lauritsen, S. Helveg, E. Lægsgaard, et al [J]. J. Catal. 2001, 197: 1.
[4] M. Chhowalla, G. A. J. Amaratunga, [J]. Nature 2000, 407: 164.
[5] I. M. Allam, [J]. J. Mater. Sci. 1991, 26:3977
[6] B. Z. Lin, C. Ding, B. H. Xu, et al [J]. Mater. Res. Bull. 2009, 44: 719.
[7] J. A. Woollam, R. B. Somoano, [J]. Phys. Rev. B 1976, 13: 3843.
[8] E. Benavente, M. A. S. Ana, F. Mendizabal, et al [J]. Coord. Chem. Rev. 2002, 224: 87.
[9] R. N. Viswanath, S. Ramasamy, [J]. J. Mater. Sci. 1990, 25:5029.
[10] P. R. Bonneau, R. F. Jarvis, R. B. Kaner, [J]. Nature 1991, 349:510.
[11] R. R. Chianelli, E.B. Restridge , T. A. Pecoraro, et al [J]. Science 1979, 203: 1105.
[12] Y. Y. Peng, Z. Y. Meng, C. Zhong, et al [J]. J. Solid State Chem. 2001, 159: 170.
[13] R. J. J. Newberry, [J]. Am. Mineral. 1979, 64: 758.
[14] A. J. Jacobson, R. R. Chianelli, M. S. Whittingham, [J]. J. Electrochem. Soc. 1979, 126: 2277.
[15] K. S. Liang, R. R. Chianelli, F. Z. Chien, et al [J]. J. Non-Crystal. Solids 1986, 79: 251.
[16] D. Yang, S. J. Sandoval, W. M. R. Divigalpitiya, et al [J]. Phys. Rev. B, 1991, 43: 12053.
[17] D. Yang, R. F. Frindt, [J]. J. Mater. Res. 1996, 11: 1733.
[18] C.M. Sung, [J]. High Temp.-High Press. 1997, 29: 253.
[19] S.M. Wang, D.W. He, W.D. Wang, et al [J]. High Pressure Res. 2009, 29: 806.
[20] F. Wypych, R. Schollhorn, [J]. J. Chem. Soc., Chem. Commun. 1992, 19: 1386.
[21] R. E. Bell, R. E. Herfert, [J]. J. Am. Chem. Soc. 1957, 79: 3351.
[22] S. M. Wang, D.W. He, in preparation.
[23] O. Kitakami, S. Okamoto, and Y. Shimada, [J]. J. Appl. Phys. 1996, 79: 6880.
[24] E. R. Leite, T. R. Giraldi, F. M. Pontes, et al [J]. Appl. Phys. Lett. 2003, 83: 1566.
[25] S. M. Wang, D. W. He, Y. T. Zou, et al [J]. J. Mater. Res. 2009, 24: 2089.
[26] Y. Zhao, J. Zhang, [J]. J. Appl. Cryst. 2008, 41: 1095.
[27] W. H. Hall, [J]. Proc. Phys. Soc. A 1949, 62: 741.
[28] G. K. Williamson, W. H. Hall, [J]. Acta Metall. 1953, 1: 22.

高压下沿（002）晶面定向生长 MoS_2 纳米晶

王善民，贺端威

（四川大学原子与分子物理研究所，成都 610065）

摘要：本文通过使用改进的高压合成腔体，成功制备了纳米晶 MoS_2，并利用 X 射线衍射和扫描电镜表征高压合成的样品。结果显示，合成的 MoS_2 样品具有纳米六方层状结构，其生长方向沿（002）最低能量晶面。另外，我们还分析了 X 射线衍射峰宽化的成因，主要的原因在于纳米晶 MoS_2 具有层与层堆积的无序性结构，传统的计算纳米晶大小及微观残余的方法，如 Scherrer 公式、Williamson-Hall 方程等，均不能用于此类因层与层堆积无序的纳米晶材料。

关键词：高压；晶体生长；缺陷；纳米结构

中图分类号：O52